



Cite this: *Analyst*, 2026, **151**, 2213

## Negative selection assisted isolation of a highly selective DNA aptamer for the detection of 17 $\alpha$ -ethinylestradiol

Nathania Lui, Qiushi Liu and Juewen Liu \*

Estrogenic compounds, including both natural estrogens such as estrone (E1) and 17 $\beta$ -estradiol (E2) and synthetic 17 $\alpha$ -ethinylestradiol (EE2), are widely recognized for their endocrine-disrupting effects in the environment. EE2 is a key ingredient in oral contraceptives, and it poses environmental challenges due to its resistance to biodegradation and bioaccumulation in aquatic systems. In this work, EE2 was used as a target to select DNA aptamers, and extensive negative selections were employed using E2 as a counter target to obtain highly selective aptamers. After 18 rounds of selections, two families of aptamers were obtained. Among them, a sequence named EE2-1 has a predicted secondary structure containing a highly conserved loop region connecting two duplex stems. EE2-1 has a  $K_d$  of 200 nM based on thioflavin T (ThT) fluorescence spectroscopy and 138 nM based on isothermal titration calorimetry. Using this ThT fluorescence assay, a limit of detection of 40 nM was determined, and its binding to E2 was much weaker. This aptamer provides a promising molecular recognition element for the development of biosensors and assays capable of detecting trace levels of EE2.

Received 30th December 2025,  
Accepted 23rd February 2026

DOI: 10.1039/d5an01374g

rsc.li/analyst

### Introduction

Estrone (E1) is a naturally occurring estrogen that supports female sexual development and function and becomes the predominant endogenous estrogen after menopause.<sup>1</sup> Another major endogenous estrogen, 17 $\beta$ -estradiol (E2), is the most potent and prevalent estrogen during the reproductive years, during which it regulates the menstrual cycle, promotes secondary sexual characteristics, and maintains reproductive tissues such as breast, uterus, and vagina. E2 is also present in lower levels in males and contributes to physiological regulation in multiple tissues. In contrast, 17 $\alpha$ -ethinylestradiol (EE2) is a synthetic derivative of E2 widely used as the estrogenic component in oral contraceptives; the ethinyl substitution at the 17 $\alpha$ -position enhances metabolic stability and oral bioavailability.<sup>2,3</sup>

Estrogenic compounds are potent environmental contaminants because they elicit endocrine-disrupting effects at nanogram-per-liter (parts per trillion) concentrations. These compounds are excreted by humans and animals and enter aquatic ecosystems through wastewater effluents and agricultural runoff, where they disrupt endocrine signaling in aquatic organisms, leading to reproductive abnormalities and population-level impacts.<sup>4</sup> The European Commission has estab-

lished strict environmental quality standards of 3.6 ng L<sup>-1</sup> for E1, 0.4 ng L<sup>-1</sup> for E2, and 0.035 ng L<sup>-1</sup> for EE2 due to their ecological risks.<sup>5</sup>

EE2 is particularly concerning due to its high potency and persistence, causing pronounced endocrine-disrupting effects even at very low concentrations.<sup>6</sup> Conventional analytical techniques for EE2, including liquid chromatography-tandem mass spectrometry (LC-MS/MS) and gas chromatography-mass spectrometry (GC-MS), are considered gold standards for estrogen quantification, with LC-MS/MS achieving detection limits down to approximately 0.02 ng L<sup>-1</sup> in water.<sup>7</sup> However, these methods typically require extensive sample preparation, derivatization for enhanced sensitivity, costly instrumentation, and highly trained personnel. Immunoassays have also been developed, but they typically require labeled or immobilized target molecules and involve competitive assays or sophisticated equipment.<sup>8-10</sup>

Aptamers are short, single-stranded DNA or RNA molecules that can fold into unique, well-defined, three-dimensional structures, enabling high-affinity and high-specificity binding to a wide variety of targets.<sup>11-14</sup> Their binding properties arise from the structure and chemical environment of the folded nucleic acid rather than simply the primary sequence, allowing discrimination between closely related molecules.<sup>15-19</sup> Aptamers can be generated *via* Systematic Evolution of Ligands by Exponential Enrichment (SELEX), an iterative process comprising cycles of target binding, removal of non-binding sequences, and amplification of binding sequences to

Department of Chemistry, Waterloo Institute for Nanotechnology, University of Waterloo, Waterloo, Ontario, N2L 3G1, Canada. E-mail: liujw@uwaterloo.ca



enrich a random oligonucleotide library for selective target binding. The resulting aptamers can be integrated into biosensing platforms and diagnostic assays for rapid, sensitive, and potentially on-site detection of target molecules in environmental samples.

E2 has been the target of numerous previous aptamer selection studies,<sup>20–25</sup> although most relied on immobilized E2, often yielding relatively long sequences without well-defined secondary structures. In our previous work, we employed a capture-SELEX strategy in which the DNA library, rather than the target, was immobilized, enabling selection against unmodified E2. Two resulting aptamers were subsequently engineered into structure-switching fluorescent biosensors capable of detecting E2 with limits of detection ranging from 3.3 to 9.1 nM.<sup>26</sup> One aptamer recognized E1, E2, and EE2, whereas the other preferentially bound E2 over EE2. Although E1, E2, and EE2 share the same steroidal core, EE2 possesses an additional ethynyl substituent at the 17 $\alpha$ -position, providing a structural feature that can be exploited for selective molecular recognition. To date, no SELEX studies have been reported using EE2 as the selection target, and only a single computational study has attempted to generate EE2-binding sequences through docking based on a previously reported E2 aptamer.<sup>27</sup> However, the resulting sequences were never validated using rigorous homogeneous binding assays,<sup>28</sup> leaving their actual affinity and specificity uncertain.

Given that aptamers capable of binding all three molecules have been reported, negative selection is essential to enrich sequences with specificity toward EE2. In this work, we employed capture-SELEX combined with extensive negative selection to isolate an aptamer that selectively binds EE2 with nanomolar affinity and high discrimination against E1 and E2. A label-free fluorescent biosensor was then developed to detect EE2 not only in buffer but also in wastewater.

## Materials and methods

### Chemicals

The DNA samples used in this study were purchased from Integrated DNA Technologies (Coralville, Iowa, USA). Streptavidin agarose resin was purchased from Fisher Scientific. E1, E2, EE2, NaCl, MgCl<sub>2</sub>, NaOH, HCl, tris(hydroxymethyl)aminomethane (Tris), and Amicon Ultra-0.5 centrifugal filter units (3000 and 10 000 molecular weight cutoffs) were from Millipore Sigma (Oakville, ON, Canada). 4-(2-Hydroxyethyl) piperazine-1-ethylsulfonic acid and sodium salt (HEPES) were from Bio Basic, Inc. (Markham, ON, Canada). SsoFast EvaGreen Supermix was purchased from Bio-Rad (Mississauga, ON, Canada). Reagents for PCR were from New England Biolabs (Ipswich, MA, USA). All buffers and solutions were prepared using Milli-Q water. The buffers included: (1) selection buffer: 20 mM Tris, pH 7.4, 500 mM NaCl, 10 mM MgCl<sub>2</sub>; and (2) separation buffer: 20 mM HEPES, pH 7.4, 250 mM NaCl. Wastewater was from the City of Kitchener, ON, Canada.

### SELEX

The selection of aptamers for EE2 followed the previously published method<sup>26</sup> and the same library and primer sequences were used as described.<sup>29</sup> In brief, a single-stranded DNA library containing a 30-nucleotide randomized region (N<sub>30</sub>) flanked by primer binding regions was annealed to a short biotinylated capture strand. A column was loaded with streptavidin-functionalized agarose beads and then washed six times with 500  $\mu$ L of selection buffer. The DNA library was loaded onto the column and cycled through the resin six times. To implement negative selection, twelve washes with 500  $\mu$ L E2 solution (200  $\mu$ M for all the rounds) were applied to the beads, followed by twelve washes with 500  $\mu$ L selection buffer; the final wash fractions were retained as background references for monitoring the selection process using quantitative PCR (qPCR). Subsequently, 750  $\mu$ L of EE2 target solution (100  $\mu$ M for rounds 1–13 and 20  $\mu$ M for rounds 14–18) was passed through the column, and the eluted DNA was collected and purified using a 3000 molecular weight cut-off (MWCO) spin column with Milli-Q water, yielding a final volume of approximately 60  $\mu$ L. The spin column was centrifuged at 14 000g five times to wash away the unbound target and concentrate the DNA pool.

The enriched pool was amplified by PCR using a biotinylated reverse primer. The PCR products were incubated with streptavidin beads, and a second column was prepared by washing with 500  $\mu$ L separation buffer and loading blank beads, which were washed six times with separation buffer. The bead–DNA complexes were cycled through this column four times and washed eight times with 500  $\mu$ L separation buffer. Single-stranded DNA was generated by adding 0.2 M NaOH to denature the duplex DNA, followed by neutralization with 0.2 M HCl. The recovered single-stranded DNA was again purified and concentrated with a 3000 MWCO spin column to approximately 60  $\mu$ L. The DNA concentration was quantified using a Spark microplate reader (Tecan) to determine input amounts for subsequent rounds. After 18 rounds of selection, the final library was subjected to deep sequencing at McMaster University.

### ThT-based fluorescence assays and detection in buffer

A Varian Eclipse fluorescence spectrophotometer was used to measure thioflavin T (ThT) fluorescence. Typical samples contained selection buffer, 1  $\mu$ M ThT, and 0.5  $\mu$ M aptamer, with a total volume of 500  $\mu$ L. Samples were transferred to a quartz cuvette, and EE2 was titrated to a final concentration of 2  $\mu$ M. The excitation wavelength was 440 nm, and emission spectra were recorded from 460 nm to 550 nm. Fluorescence intensity at 490 nm was used for data analysis. Apparent dissociation constants ( $K_d$ ) were obtained by fitting the binding curve to

$$F = F_0 + aK_d / (K_d + [C])$$

where [C] is the target concentration, and  $a$  is the maximal signal change at saturated binding.



## Isothermal titration calorimetry

Isothermal titration calorimetry (ITC) was performed using a MicroCal VP-ITC. Aptamer and target solutions were prepared in selection buffer; DNA samples were annealed, cooled to room temperature, and degassed for 5 min prior to loading. 10  $\mu\text{M}$  solution of the aptamer and 100  $\mu\text{M}$  of the target (EE2) were taken in a syringe at 25  $^{\circ}\text{C}$ . 10  $\mu\text{L}$  EE2 was injected each time, except for the initial 0.5  $\mu\text{L}$  injection. The resulting heat changes were integrated and plotted as a function of the molar ratio of EE2 to aptamer, and the data were fitted to a one-site model using Origin software to obtain thermodynamic parameters.

## Detection of EE2 in wastewater

Wastewater from Kitchener, ON, Canada, was used as a representative real-water matrix. The same salt and buffer were added to the wastewater sample, and the final wastewater content of the sample was approximately 90% of the total volume. ThT-based fluorescence assays were conducted as described above, except that a tap water buffer was formulated using tap water in place of Milli-Q water, while maintaining the same component concentrations and volumes.

# Results and discussion

## Capture-SELEX with negative selections for EE2 aptamers

To select aptamers for EE2, we used the capture-SELEX method in this work,<sup>30,31</sup> and the DNA library consisted of an  $N_{30}$  randomized region flanked by constant primer binding regions. Since our previous selection using E2 as a target

yielded aptamers that can bind to both E2 and EE2,<sup>26</sup> a negative selection step was incorporated here using 200  $\mu\text{M}$  E2 as a counter target prior to introducing EE2. Thirteen rounds of selection were performed with 100  $\mu\text{M}$  EE2, followed by five rounds with 20  $\mu\text{M}$  EE2, for a total of 18 rounds. Real-time PCR monitoring indicated substantial enrichment of binding sequences by round 13. Deep sequencing of the round 18 pool yielded 58 746 reads.

The final library was well converged, and the ten most abundant sequences were clustered into two families along with a few ungrouped sequences. The  $N_{30}$  regions are aligned as shown in Fig. 1A. Family 1 is the dominating family accounting for 57% of the total reads, and the most abundant sequence EE2-1 represented approximately one third of the library. Family 1 is featured with the conserved nucleotides in red. Family 2 occupied nearly 31% of the library and its representative sequence is EE2-2. The conserved region in Family 2 is shorter as marked by the blue color. Therefore, the EE2-1 and EE2-2 aptamers were picked for further functional characterization to identify the most selective EE2 binder. As illustrated in Fig. 1C, both aptamers adopt a structure consisting of two stem regions connected by a loop containing conserved nucleotides, which are likely responsible for target binding.

## ThT fluorescence-based binding assays

To evaluate the binding properties of the aptamers, we first used thioflavin T (ThT) as a fluorescent probe. ThT-based fluorescence assays provide a convenient means to probe aptamer selectivity because ThT fluorescence responds sensitively to changes in the nucleic acid structure. ThT is a benzothiazole dye that becomes strongly fluorescent upon binding to struc-

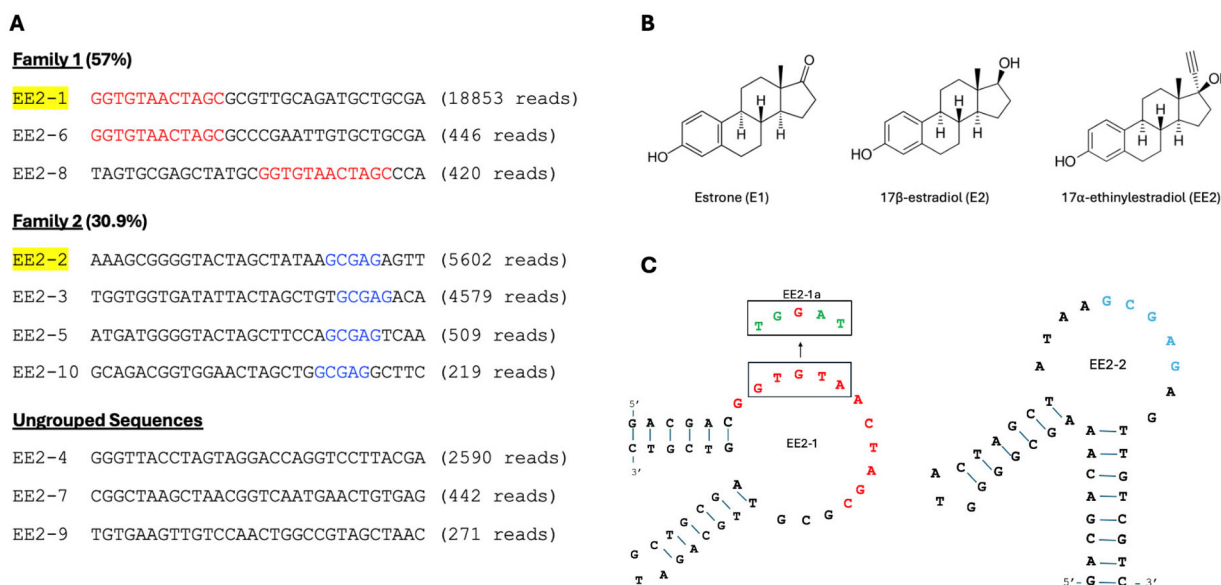


**Fig. 1** (A) Alignment of the  $N_{30}$  region of the top 10 most abundant sequences in the round 18 library. The conserved sequences are shown in red or blue. The number of reads is out of a total of 58 746 sequences. The most abundant sequence in each family is highlighted in yellow. (B) Structures of E1, E2, and EE2. (C) Secondary structures of aptamers EE2-1 and EE2-2. A mutant of EE2-1 named EE2-1a is also shown, where the mutated bases are in green.



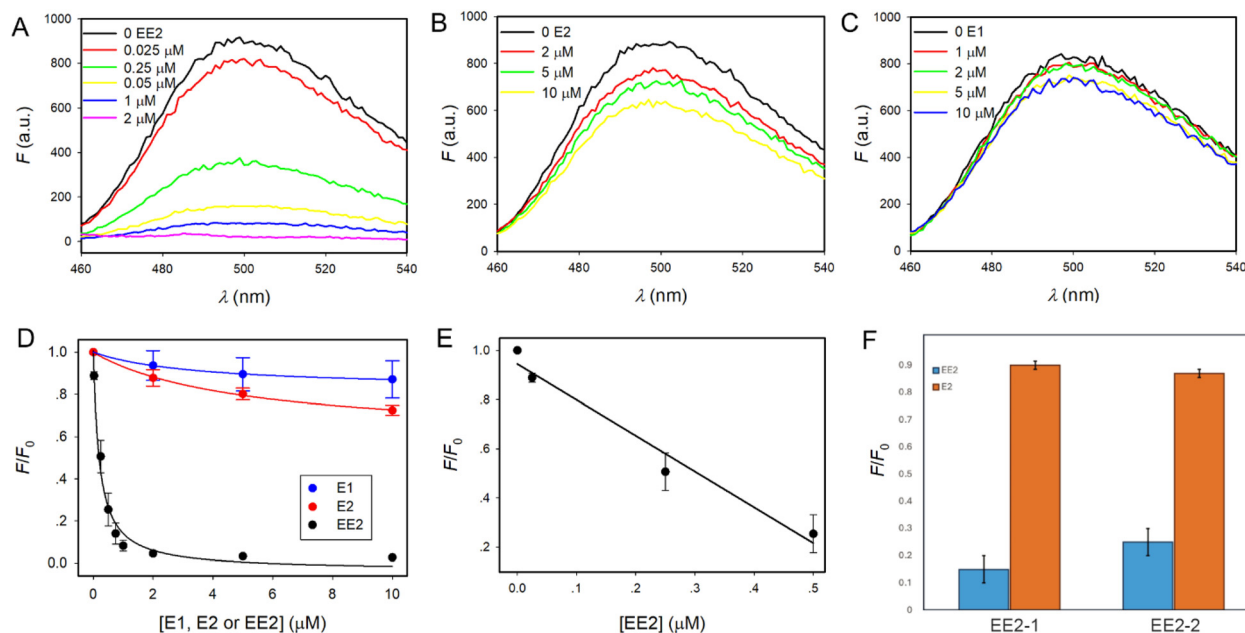


**Fig. 2** Fluorescence spectra of 1  $\mu\text{M}$  ThT mixed with 0.5  $\mu\text{M}$  EE2-1 aptamer titrated with increasing concentrations of (A) EE2, (B) E2 and (C) E1. (D) Binding curves of the EE2-1 aptamer for the three compounds based on the ThT fluorescence assays. (E) Initial linear response of the EE2-1 aptamer to low concentrations of EE2 for the determination of the LOD. (F) Comparison of the EE2-1 or EE2-2 aptamers after adding 1  $\mu\text{M}$  E2 or EE2. The error bars indicate the standard deviation from three repetitions.

tured DNA;<sup>32</sup> target binding can displace ThT or alter its binding environment, resulting in a measurable fluorescence change that reflects aptamer–target interactions. Compared to other dyes, ThT has weaker interactions with DNA and thus perturbs less of aptamer binding to targets.<sup>28,33</sup>

We first mixed 0.5  $\mu\text{M}$  EE2-1 aptamer with 1  $\mu\text{M}$  ThT, which produced a fluorescence emission peak at approximately 490 nm. Upon titration with EE2, the fluorescence was nearly completely quenched (Fig. 2A), indicating aptamer binding to EE2. The pronounced quenching further demonstrates that ThT serves as an effective fluorescent probe in this system. In contrast, titration with E2 (Fig. 2B) or E1 (Fig. 2C) caused only minor decreases in fluorescence, confirming the selective binding of the aptamer to EE2. The fraction of fluorescence decrease was subsequently plotted and fitted to a one-site binding model, yielding an apparent  $K_d$  of 200 nM (Fig. 2D). This  $K_d$  value may be underestimated, as 500 nM aptamer was used in the assay, placing the system in the titration regime ( $K_d \cong$  half of the aptamer concentration).<sup>34,35</sup> Binding for E2 or E1 cannot be fitted due to the small amount of fluorescence change in those samples.

Given the substantial fluorescence quenching observed, this ThT-based assay can be readily adapted as a label-free fluorescent biosensor for EE2 detection. By plotting the initial linear response and analyzing the signal decrease, the limit of detection (LOD) was determined to be 40 nM, calculated based on a signal exceeding three times the standard deviation of the background noise.

We further evaluated the response of the EE2-2 aptamer in the presence of 1  $\mu\text{M}$  EE2 or 1  $\mu\text{M}$  E2 (Fig. 2F). Consistent with

EE2-1, this aptamer also demonstrated preferential binding to EE2 over E2. However, EE2-1 induced a more substantial fluorescence decrease than EE2-2, indicating a stronger affinity toward EE2. Accordingly, subsequent investigations were conducted using the EE2-1 aptamer.

### Mutation and effect of $\text{Mg}^{2+}$

To further validate the sensitivity and specificity of EE2-1, a mutant sequence (EE2-1a) was designed as shown in Fig. 1C, in which several nucleotides within the conserved region were rearranged. This mutant exhibited no EE2-dependent fluorescence change (Fig. 3A), indicating a loss of binding. This control experiment confirms that EE2-1 is a true aptamer and that target recognition involves the conserved loop region.

Many aptamers require divalent metal ions, such as  $\text{Mg}^{2+}$ ,<sup>36,37</sup> to maintain their binding structure. Because 10 mM  $\text{Mg}^{2+}$  was present in both the selection buffer and the above binding assays, we also evaluated binding in a buffer completely devoid of  $\text{Mg}^{2+}$ . The resulting binding curve overlapped fully with that obtained in the presence of  $\text{Mg}^{2+}$ , demonstrating that EE2-1 binds EE2 independently of  $\text{Mg}^{2+}$ . This  $\text{Mg}^{2+}$ -independent binding may be attributed to the hydrophobic nature of EE2, suggesting that metal-ion-mediated bridging is not required for target recognition. The  $\text{Mg}^{2+}$ -independent binding also makes EE2-1 a robust aptamer for applications in various buffer conditions.

### ITC characterization for EE2 binding

The  $K_d$  determined from the ThT fluorescence assay represents an apparent value, as ThT may interfere with target binding.<sup>28</sup> To obtain a more accurate measurement and detailed thermo-



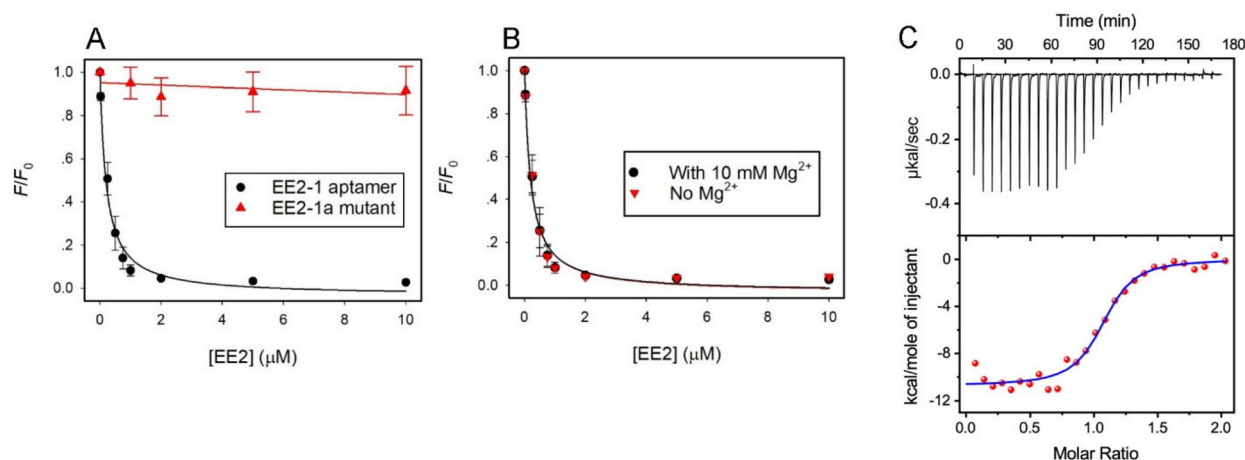


**Fig. 3** (A) The EE2-1a mutant cannot bind to EE2 based on the ThT fluorescence assay. (B)  $\text{Mg}^{2+}$  did not affect the binding of the EE2-1 aptamer. (C) The ITC binding analysis of titrating 100  $\mu\text{M}$  EE2 into 10  $\mu\text{M}$  EE2-1 aptamer.

dynamic information, isothermal titration calorimetry (ITC) was employed to characterize the interaction between EE2 and EE2-1. ITC directly measures the heat released or absorbed during complex formation, providing the binding affinity, enthalpy ( $\Delta H$ ), entropy ( $\Delta S$ ), Gibbs free energy ( $\Delta G$ ), and binding stoichiometry ( $N$ ) in a single, label-free experiment performed in solution, thereby preserving native binding behavior.<sup>38</sup>

In the ITC experiment, 10  $\mu\text{M}$  EE2-1 was placed in the sample cell and titrated with 100  $\mu\text{M}$  EE2 at 25 °C. Each injection of EE2 produced an exothermic heat signal, and integration of the heat

pulses generated a binding isotherm (Fig. 3C). Fitting the data to a one-site binding model yielded a  $K_d$  of 138 nM, confirming strong nanomolar affinity. The binding was characterized by a  $\Delta H$  of  $-10.7 \text{ kcal mol}^{-1}$  and a  $\Delta S$  of  $-4.62 \text{ cal K}^{-1} \text{ mol}^{-1}$ , indicating an enthalpy-driven binding. To put this binding affinity into perspective, a previous study reported that nonspecific EE2-DNA interactions occur with a dissociation constant on the order of 1 mM.<sup>39</sup> In contrast, the EE2-1 aptamer binds EE2 approximately four orders of magnitude stronger, highlighting the dramatic enhancement in affinity achieved through selective aptamer evolution.

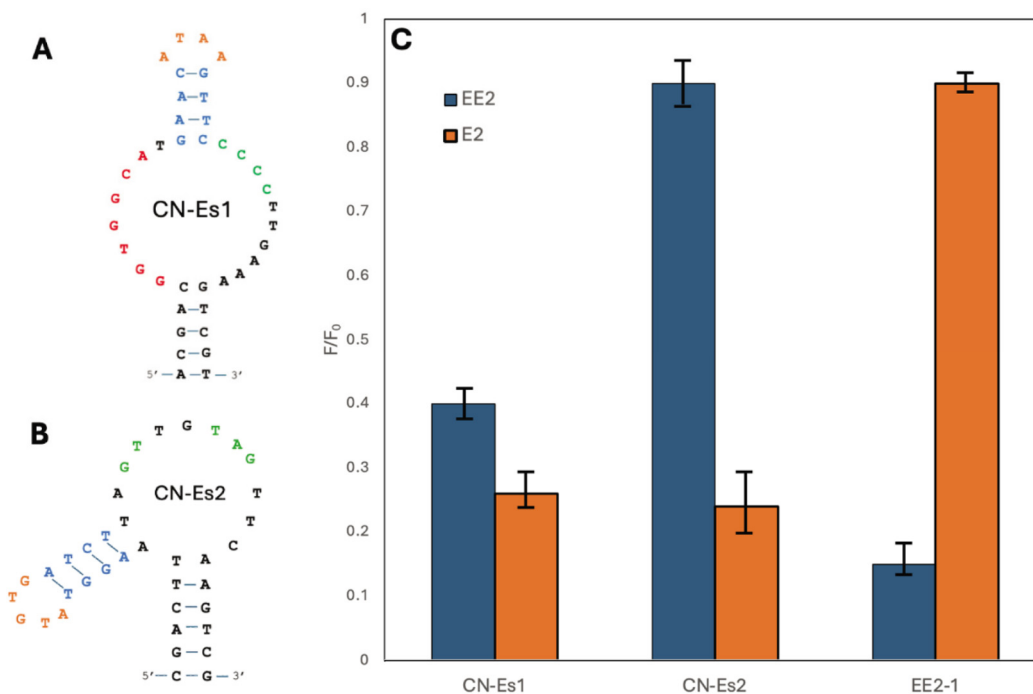


**Fig. 4** The secondary structures of the (A) CN-Es1 and (B) CN-Es2 aptamers from previous selection. (C) ThT-based fluorescence binding comparison between two previous aptamers, CN-Es1 and CN-Es2, against E2 and EE2. The error bars indicate the standard deviation from three repetitions.



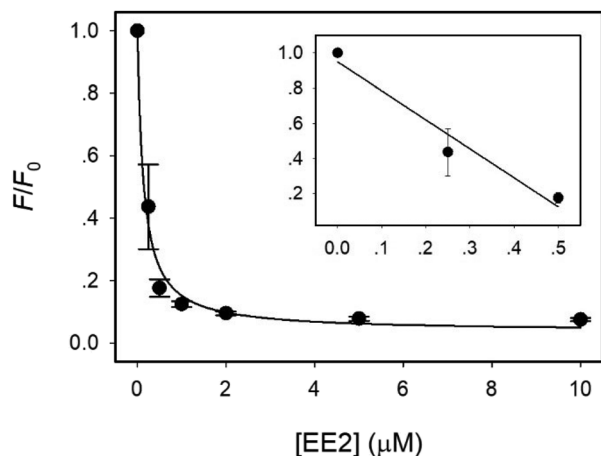


**Fig. 5** ThT-based fluorescence binding assay in wastewater. Insets: the linear range and the regression line at low EE2 concentrations. The error bars indicate the standard deviation from three repetitions.

### Comparison with previous aptamers

A previous study from our lab identified two E2-binding aptamers, CN-Es1 and CN-Es2 (Fig. 4A and B). CN-Es1 functions as a broader-spectrum aptamer capable of recognizing E1, E2, and EE2, whereas CN-Es2 is more selective for E2.<sup>26</sup> To benchmark the performance of the EE2-1 aptamer, we employed the same ThT fluorescence assay used for CN-Es1 and CN-Es2, testing responses to 2  $\mu\text{M}$  E2 or 2  $\mu\text{M}$  EE2 (Fig. 4C). Both CN-Es1 and CN-Es2 exhibited strong fluorescence enhancement in the presence of E2, confirming their sensitivity toward the natural estrogen.

In contrast, when challenged with EE2, CN-Es1 produced a reduced fluorescence signal, and CN-Es2 showed virtually no response, consistent with our previous findings that CN-Es2 does not effectively bind EE2.<sup>26</sup> Notably, when responding to 2  $\mu\text{M}$  EE2, EE2-1 generated a larger signal change than CN-Es1, indicating improved sensitivity toward EE2 under the assay conditions. Together, these results highlight the superior suitability of EE2-1 for the selective detection of EE2.

### Detection of EE2 in wastewater

To evaluate the robustness of EE2-1 in real matrices, the ThT-based fluorescence assays were conducted in a buffer prepared using wastewater. The EE2-1 aptamer retained its ability to bind EE2 at low concentrations in this very challenging matrix, and the titration behaviour closely resembled that observed in selection buffer with an apparent  $K_d$  of 140 nM and a LOD of 250 nM (Fig. 5). Such a robust performance can be attributed to its  $\text{Mg}^{2+}$ -independent binding. These findings support the potential application of EE2-1 in monitoring EE2 in environmental waters.

## Conclusion

In this work, we employed a SELEX strategy incorporating negative selection against E2 to obtain a highly selective DNA

aptamer for EE2. This approach yielded the EE2-1 aptamer, which binds EE2 with a dissociation constant of 138 nM as determined using ITC while exhibiting negligible cross-reactivity with E2 and E1, confirming its specificity. The identification of an EE2-specific aptamer with both high affinity and selectivity represents an important advance toward molecular recognition elements for environmental monitoring of endocrine-disrupting compounds. The label-free ThT fluorescence assay developed here serves as a convenient proof-of-concept sensing platform, demonstrating that EE2-1 can produce a measurable fluorescence response without the need for chemical labeling. More sensitive detection schemes could be achieved by integrating alternative signal transduction mechanisms.<sup>40–43</sup> Looking ahead, the incorporation of EE2-1 into portable sensor formats, such as electrochemical, colorimetric, or paper-based devices, offers a promising path toward rapid, on-site detection of EE2 in environmental samples.

## Conflicts of interest

There are no conflicts to declare.

## Data availability

The data that support the findings of this study are available from the the Federated Research Data Repository, at <https://doi.org/10.20383/103.01574>.

## Acknowledgements

The authors acknowledge funding for this work from the Government of Canada's New Frontiers in Research Fund (NFRF), the Natural Sciences and Engineering Research Council of Canada (NSERC) and the Canada Research Chairs program.

## References

- 1 E. Diamanti-Kandarakis, J.-P. Bourguignon, L. C. Giudice, R. Hauser, G. S. Prins, A. M. Soto, R. T. Zoeller and A. C. Gore, *Endocr. Rev.*, 2009, **30**, 293–342.
- 2 M. Klaic and F. Jirsa, *RSC Adv.*, 2022, **12**, 12794–12805.
- 3 A. Z. Aris, A. S. Shamsuddin and S. M. Praveena, *Environ. Int.*, 2014, **69**, 104–119.
- 4 K. A. Kidd, P. J. Blanchfield, K. H. Mills, V. P. Palace, R. E. Evans, J. M. Lazorchak and R. W. Flick, *Proc. Natl. Acad. Sci. U. S. A.*, 2007, **104**, 8897–8901.
- 5 Y. Luo, W. Guo, H. H. Ngo, L. D. Nghiem, F. I. Hai, J. Zhang, S. Liang and X. C. Wang, *Sci. Total Environ.*, 2014, **473–474**, 619–641.
- 6 H. Chang, Y. Wan, S. Wu, Z. Fan and J. Hu, *Water Res.*, 2011, **45**, 732–740.
- 7 C. Ripollés, M. Ibáñez, J. V. Sancho, F. J. López and F. Hernández, *Anal. Methods*, 2014, **6**, 5028–5037.



- 8 H. Kanson, N. Inguibert, G. Istamboulie, L. Barthelmebs, C. Calas-Blanchard and T. Noguier, *Anal. Biochem.*, 2017, **537**, 63–68.
- 9 Y. Li, Y. Zhang, S. Ru, Z. Zhang, Z. Yue and J. Wang, *Talanta*, 2023, **254**, 124135.
- 10 R. Hamid, Y. Mustapha Kamil, A. Z. Aris, M. H. Abu Bakar, F. H. Suhailin, M. T. Alresheedi, E. K. Ng and M. A. Mahdi, *Measurement*, 2024, **238**, 115305.
- 11 L. Wu, Y. Wang, X. Xu, Y. Liu, B. Lin, M. Zhang, J. Zhang, S. Wan, C. Yang and W. Tan, *Chem. Rev.*, 2021, **121**, 12035–12105.
- 12 S. Qian, D. Chang, S. He and Y. Li, *Anal. Chim. Acta*, 2022, **1196**, 339511.
- 13 M. Famulok and G. Mayer, *Chem. Biol.*, 2014, **21**, 1055–1058.
- 14 K.-Y. Wong, M.-S. Wong, J. H. Lee and J. Liu, *Adv. Drug Delivery Rev.*, 2025, **224**, 115646.
- 15 N. Nakatsuka, K. A. Yang, J. M. Abendroth, K. M. Cheung, X. Xu, H. Yang, C. Zhao, B. Zhu, Y. S. Rim, Y. Yang, P. S. Weiss, M. N. Stojanović and A. M. Andrews, *Science*, 2018, **362**, 319–324.
- 16 S. Stangherlin, N. Lui, J. H. Lee and J. Liu, *TrAC, Trends Anal. Chem.*, 2025, **191**, 118349.
- 17 O. Alkhamis, J. Canoura, H. Yu, Y. Liu and Y. Xiao, *TrAC, Trends Anal. Chem.*, 2019, **121**, 115699.
- 18 A. Ruscito and M. C. DeRosa, *Front. Chem.*, 2016, **4**, 14.
- 19 Y. Ding and J. Liu, *Chin. J. Chem.*, 2024, **42**, 2391–2400.
- 20 Y. S. Kim, H. S. Jung, T. Matsuura, H. Y. Lee, T. Kawai and M. B. Gu, *Biosens. Bioelectron.*, 2007, **22**, 2525–2531.
- 21 O. A. Alsager, S. Kumar, G. R. Willmott, K. P. McNatty and J. M. Hodgkiss, *Biosens. Bioelectron.*, 2014, **57**, 262–268.
- 22 K. Vanschoenbeek, J. Vanbrabant, B. Hosseinkhani, V. Vermeeren and L. Michiels, *J. Steroid Biochem. Mol. Biol.*, 2015, **147**, 10–16.
- 23 S. U. Akki, C. J. Werth and S. K. Silverman, *Environ. Sci. Technol.*, 2015, **49**, 9905–9913.
- 24 M. Jauset-Rubio, M. L. Botero, V. Skouridou, G. B. Aktas, M. Svobodova, A. S. Bashammakh, M. S. El-Shahawi, A. O. Alyoubi and C. K. O'Sullivan, *ACS Omega*, 2019, **4**, 20188–20196.
- 25 K.-A. Yang, R. Pei, D. Stefanovic and M. N. Stojanovic, *J. Am. Chem. Soc.*, 2012, **134**, 1642–1647.
- 26 C. Niu, C. Zhang and J. Liu, *Environ. Sci. Technol.*, 2022, **56**, 17702–17711.
- 27 N. Rozi, S. Abu Hanifah, R. Abdulmalek Hassan, N. Huda Abdul Karim, M. Ikeda, N. N. Mansor, T. Kok Mun and T. A. P. Arputheraj, *Microchem. J.*, 2024, **205**, 111325.
- 28 S. Stangherlin, Y. Ding and J. Liu, *Small Methods*, 2025, **9**, 2401572.
- 29 J. Wang, X. Li, H. Lei and J. Liu, *Analyst*, 2024, **149**, 5482–5490.
- 30 R. Nutiu and Y. Li, *Angew. Chem., Int. Ed.*, 2005, **44**, 1061–1065.
- 31 K.-A. Yang, R. Pei and M. N. Stojanovic, *Methods*, 2016, **106**, 58–65.
- 32 F. Yeasmin Khusbu, X. Zhou, H. Chen, C. Ma and K. Wang, *TrAC, Trends Anal. Chem.*, 2018, **109**, 1–18.
- 33 Y. Shu, S. Liu and J. Liu, *Anal. Chem.*, 2025, **97**, 19767–19774.
- 34 I. Jarmoskaite, I. AlSadhan, P. P. Vaidyanathan and D. Herschlag, *eLife*, 2020, **9**, e57264.
- 35 A. T. H. Le, S. M. Krylova and S. N. Krylov, *ACS Sens.*, 2026, **11**, 779–791.
- 36 P.-J. J. Huang and J. Liu, *Angew. Chem., Int. Ed.*, 2023, **62**, e202212879.
- 37 L. Gu, H. Zhang, Y. Ding, Y. Zhang, D. Wang and J. Liu, *Smart Mol.*, 2023, **1**, e20230007.
- 38 S. Slavkovic and P. E. Johnson, *Aptamers*, 2018, **2**, 45–51.
- 39 J. Sochr, K. Nemčková, M. Černicová, K. Campbell, V. Milata, D. Farkašová and J. Labuda, *Electroanalysis*, 2019, **31**, 1961–1968.
- 40 Y. Ma, W. Lewis, P. Yan, X. Shao, Q. Mou, L. Kong, W. Guo and Y. Lu, *Chem. Sci.*, 2025, **16**, 8023–8029.
- 41 J. Nie, L. Yuan, K. Jin, X. Han, Y. Tian and N. Zhou, *Biosens. Bioelectron.*, 2018, **122**, 254–262.
- 42 H. Song, D. H. Jung, Y. Cho, H. H. Cho, V. G. Panferov, J. Liu, J. H. Heo and J. H. Lee, *Coord. Chem. Rev.*, 2025, **541**, 216835.
- 43 W. T. Xu, W. C. He, Z. H. Du, L. Y. Zhu, K. L. Huang, Y. Lu and Y. B. Luo, *Angew. Chem., Int. Ed.*, 2021, **60**, 6890–6918.

